

# Structural development of cortical bone morphology in the human femoral and tibial diaphyses indicates age- and site-specific biomechanical competence

Zachariah R. Hubbell<sup>1</sup>, James H. Gosman<sup>1</sup>, Colin N. Shaw<sup>2</sup>, Timothy M. Ryan<sup>3,4</sup>

<sup>1</sup>Department of Anthropology, The Ohio State University; <sup>2</sup>McDonald Institute for Archaeological Research, Cambridge University; <sup>3</sup>Department of Anthropology, Pennsylvania State University; <sup>4</sup>Center for Quantitative Imaging, EMS Energy Institute, Pennsylvania State University

## BACKGROUND

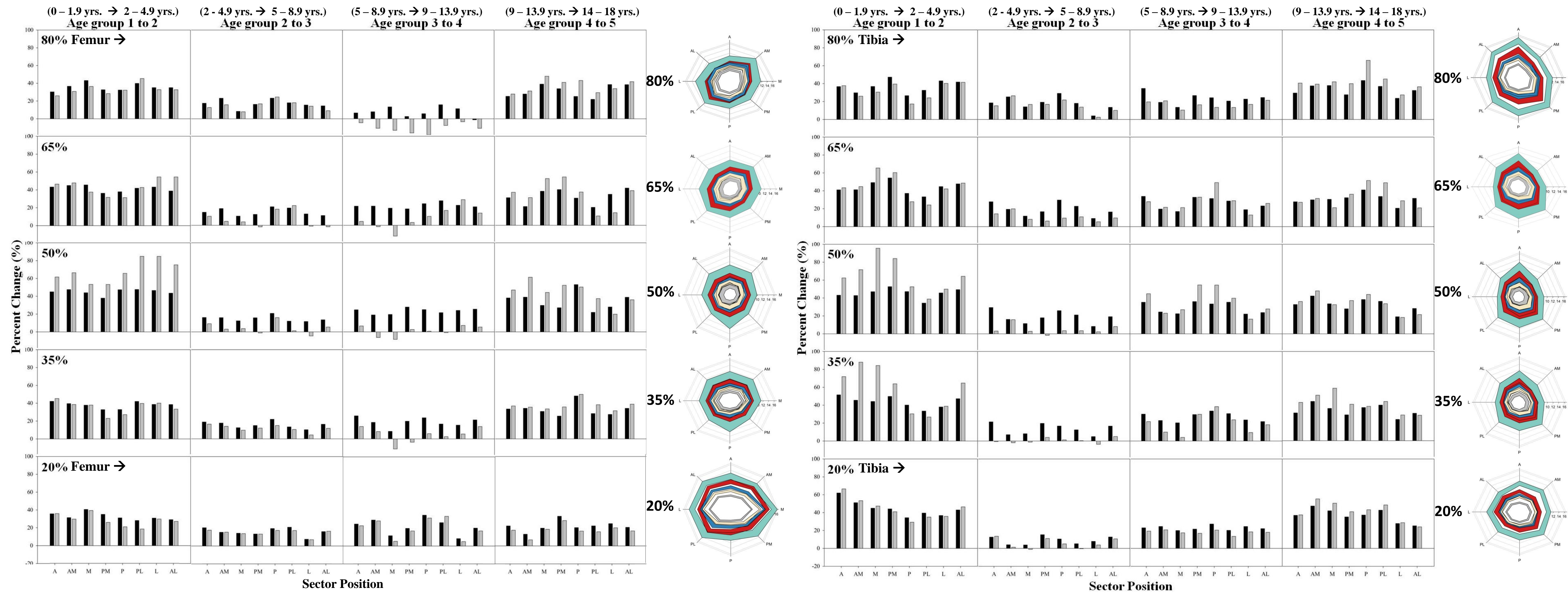
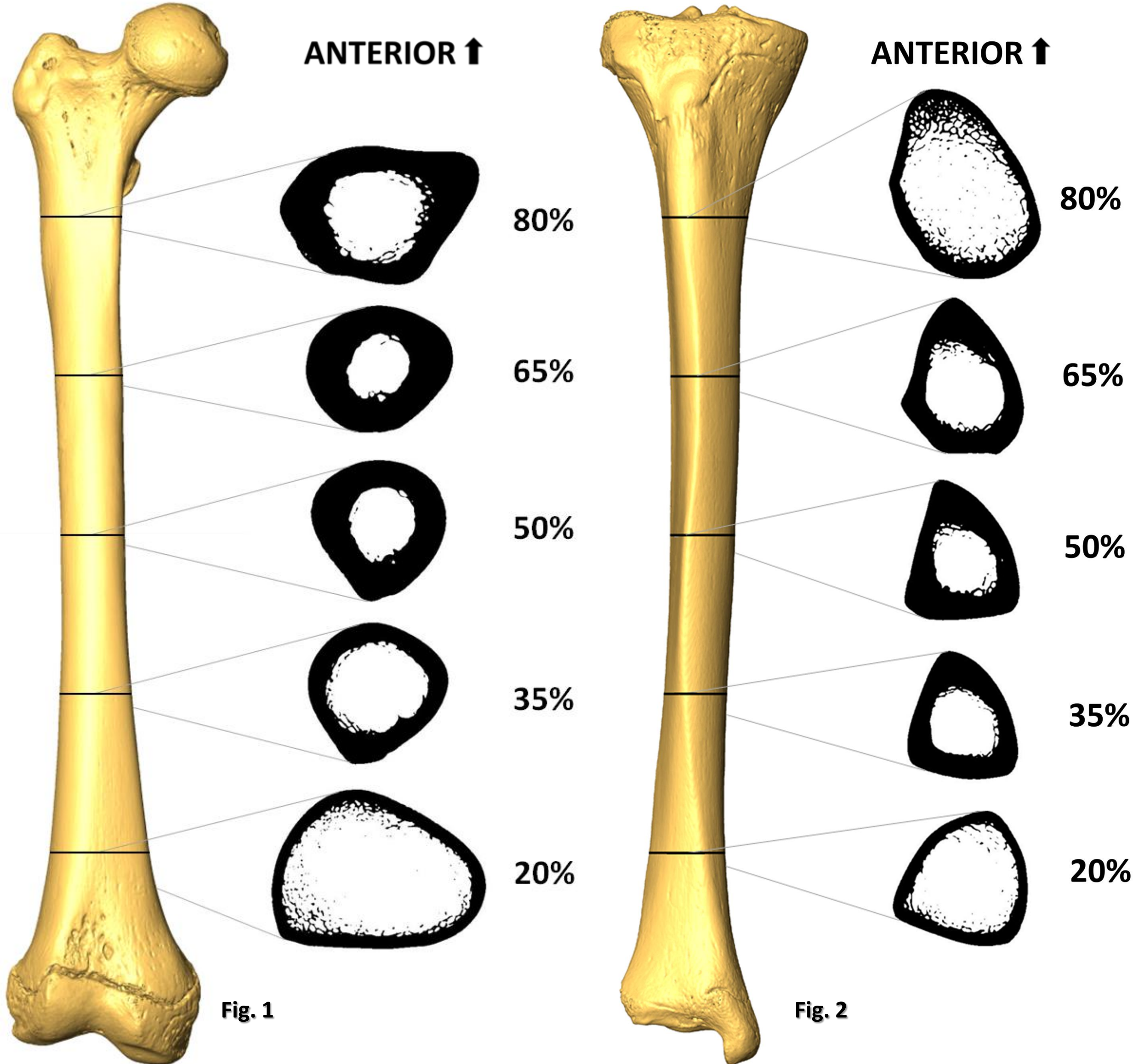
- Developmental structural differentiation in human long bone morphology is a key element in the variability of adult long bone structure.
- Dimensional scaling methods currently used for determining subadult injury thresholds assume geometric similarity between children and adults.<sup>1</sup>
- Given the unique biomechanical demands of locomotor ontogeny and longitudinal growth, a more nuanced understanding of the developmental timing and spatial variability of long bone morphological characteristics is needed in order to develop accurate child response targets.
- HYPOTHESIS:** Ontogenetic patterns of cross sectional cortical shape change in the human femoral and tibial diaphyses are age- and anatomical site-specific.

## MATERIALS

- Human femora (n=46) and tibiae (n=47).
- Ages range from neonatal to 16.5 years.
- Bones obtained from the Norris Farms #36 series, an Oneota Native American skeletal assemblage dating to about A.D. 1300.
- High resolution x-ray CT scans were taken at the Pennsylvania State Center for Quantitative Imaging.
- CT scan resolutions range from 0.013mm to 0.094mm, depending on specimen size (with higher resolutions for smaller bones).

## METHODS

- Cortical drift patterns and relative bone envelope modeling activity were assessed across age groups in five locations per bone (at 20, 35, 50, 65, and 80% of total bone length [Figs. 1 & 2]) by measuring the distance from the section centroid to the endosteal and periosteal margins in eight cross-sectional sectors using ImageJ (Figs. 4, 5, & 6).
- Changes in the periosteal and/or endosteal surfaces and in cortical width were recorded for each of the five diaphyseal slices (per bone).
- Correlation between age and  $I_{max}/I_{min}$  ratio was tested at each slice location (Fig. 3).



**Figs 9 & 10 (above).** Percent change (with age) in mean cross-sectional radius in each sector for femora (left) and tibiae (right). Black bars = periosteal change; grey bars = endosteal change. Radial graphs show mean cross-sectional radii for all age groups, plotted separately for each slice location.

## RESULTS

- Cortical shape changes are most strongly associated with age in the distal (20% total bone length) and proximal (80% total bone length) regions of the *femoral* diaphysis, and in the proximal regions (65% and 80% total bone length) of the *tibia* (Pearson correlation results in *Tables 1 & 2*).
- This indicates that these anatomical locations may be more sensitive to developmental mechanical load shifts than the midshaft (50% length).
- Age-specific mean  $I_{max}/I_{min}$  values at 5 shaft locations are shown in *Figs. 7 & 8*.
- Bone surface changes are highly age- and site-specific, with accelerated periods of change identified in the early childhood and pre-pubertal stages of development (Figs. 9 & 10).

1	I <sub>max</sub> /I <sub>min</sub> vs Age (FEMUR)				
Slice	20%	35%	50%	65%	80%
r	-0.665	-0.358	0.038	0.599	0.365
p-value	<0.001	<0.01	NS	<0.001	<0.01

2	I <sub>max</sub> /I <sub>min</sub> vs Age (TIBIA)				
Slice	20%	35%	50%	65%	80%
r	-0.417	0.792	0.825	0.880	0.859
p-value	<0.01	<0.001	<0.001	<0.001	<0.001

**Tables 1 & 2.** Pearson correlation results for  $I_{max}/I_{min}$  and age in the femur (left table) and in the tibia (right table) at each of the five slice locations per bone. Red significance values indicate significant p-values after Bonferroni correction (corrected p=0.005).

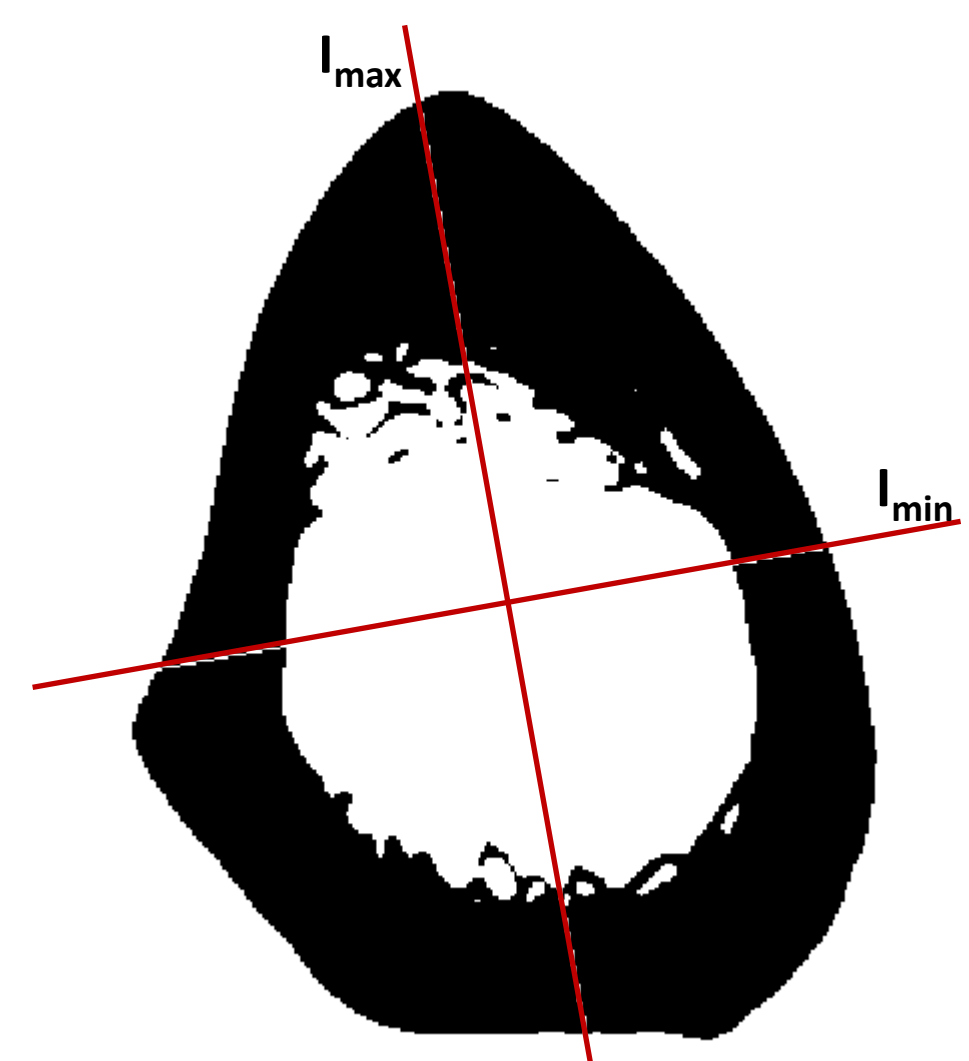


**Fig 3.** Second moments of area representing axes of maximum ( $I_{max}$ ) and minimum ( $I_{min}$ ) bending rigidity. The ratio of these values is an index of shape (1=symmetrical; 0=asymmetrical).

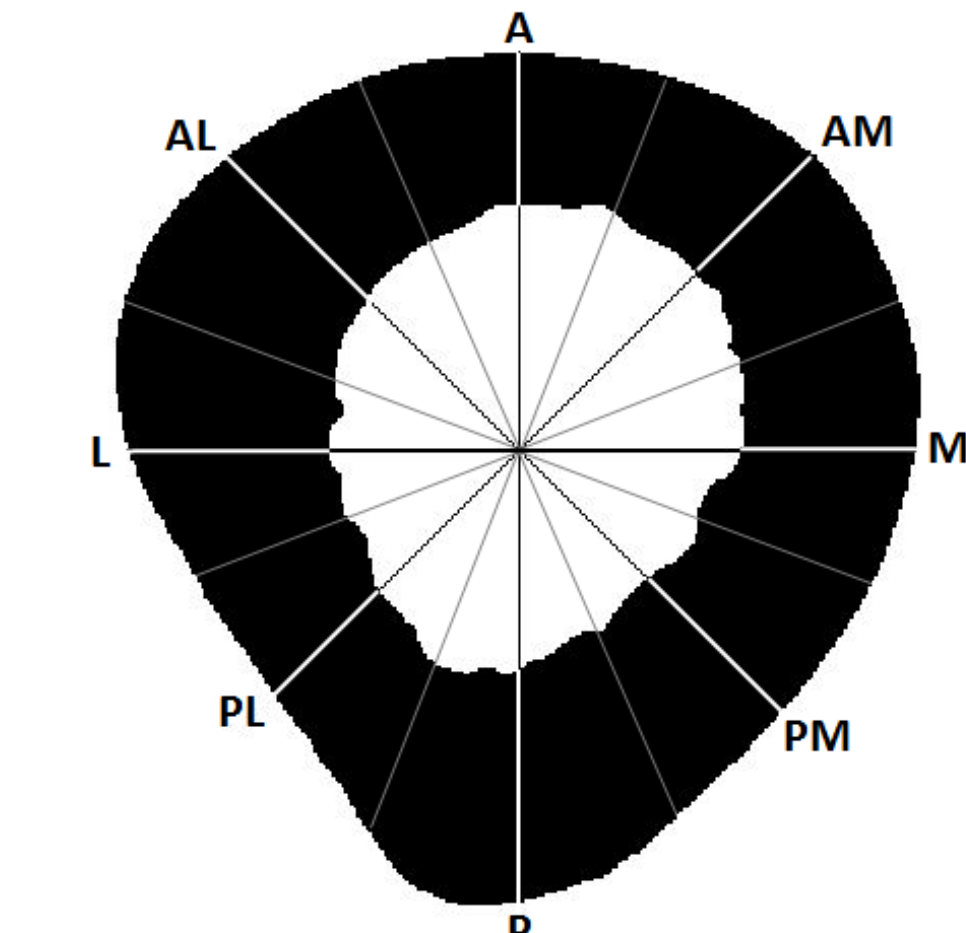


**Fig 4.** Cross section with radial grid. Gray lines designate 8 sectors. White lines bisect sectors. Letters are directional indicators.

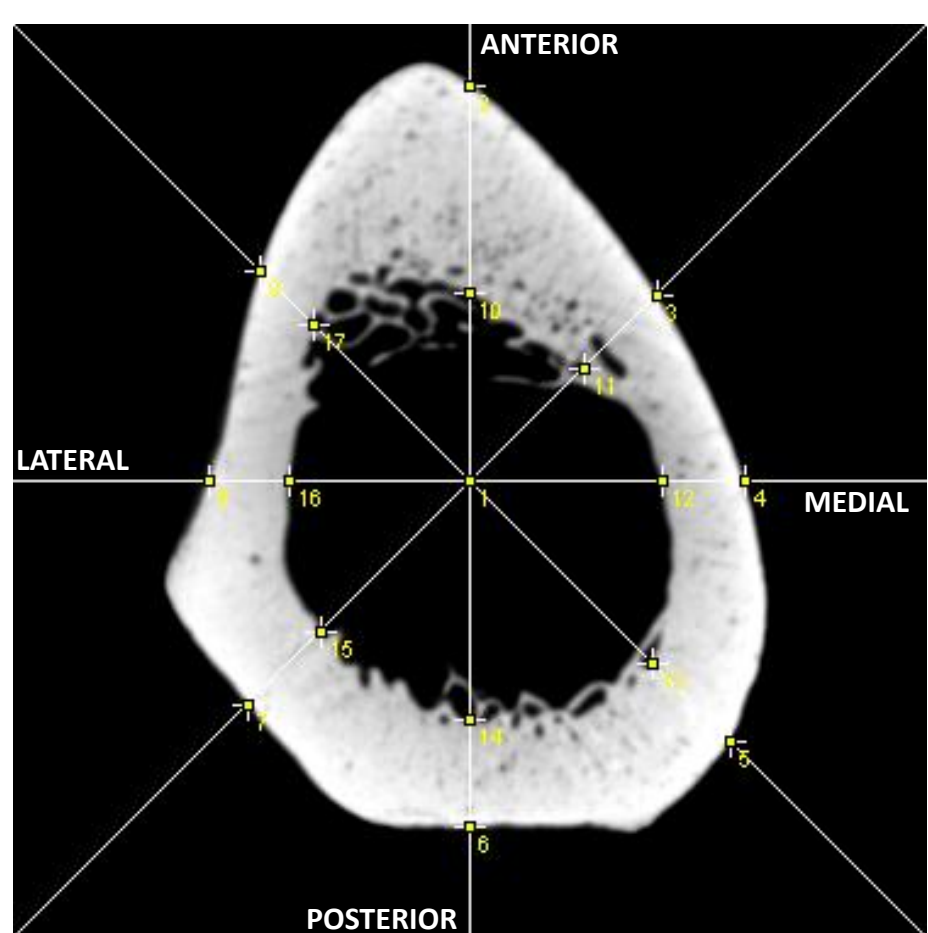


**Fig 5.** Tibial cross section at 80% length. Centered radial grid intersects cortical surfaces in 16 locations (twice per sector). Age = 16.5 yrs.

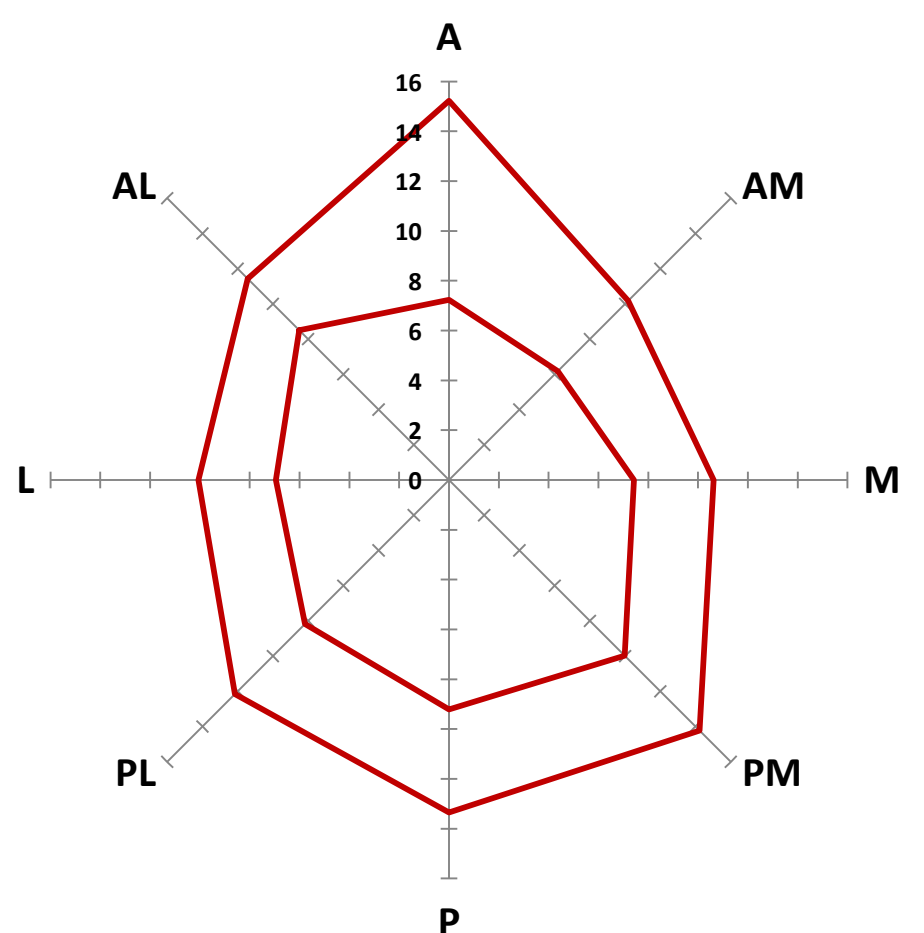
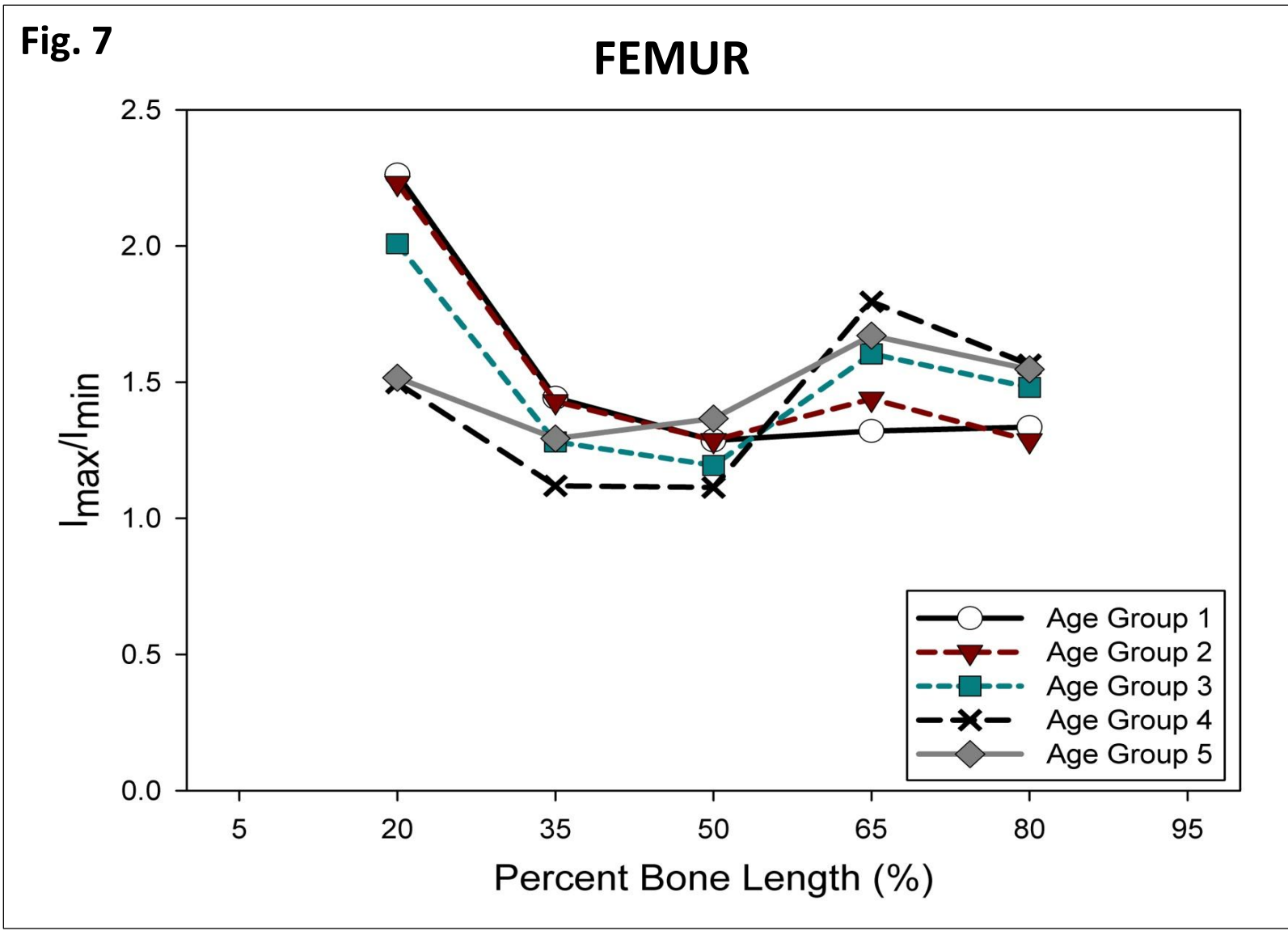
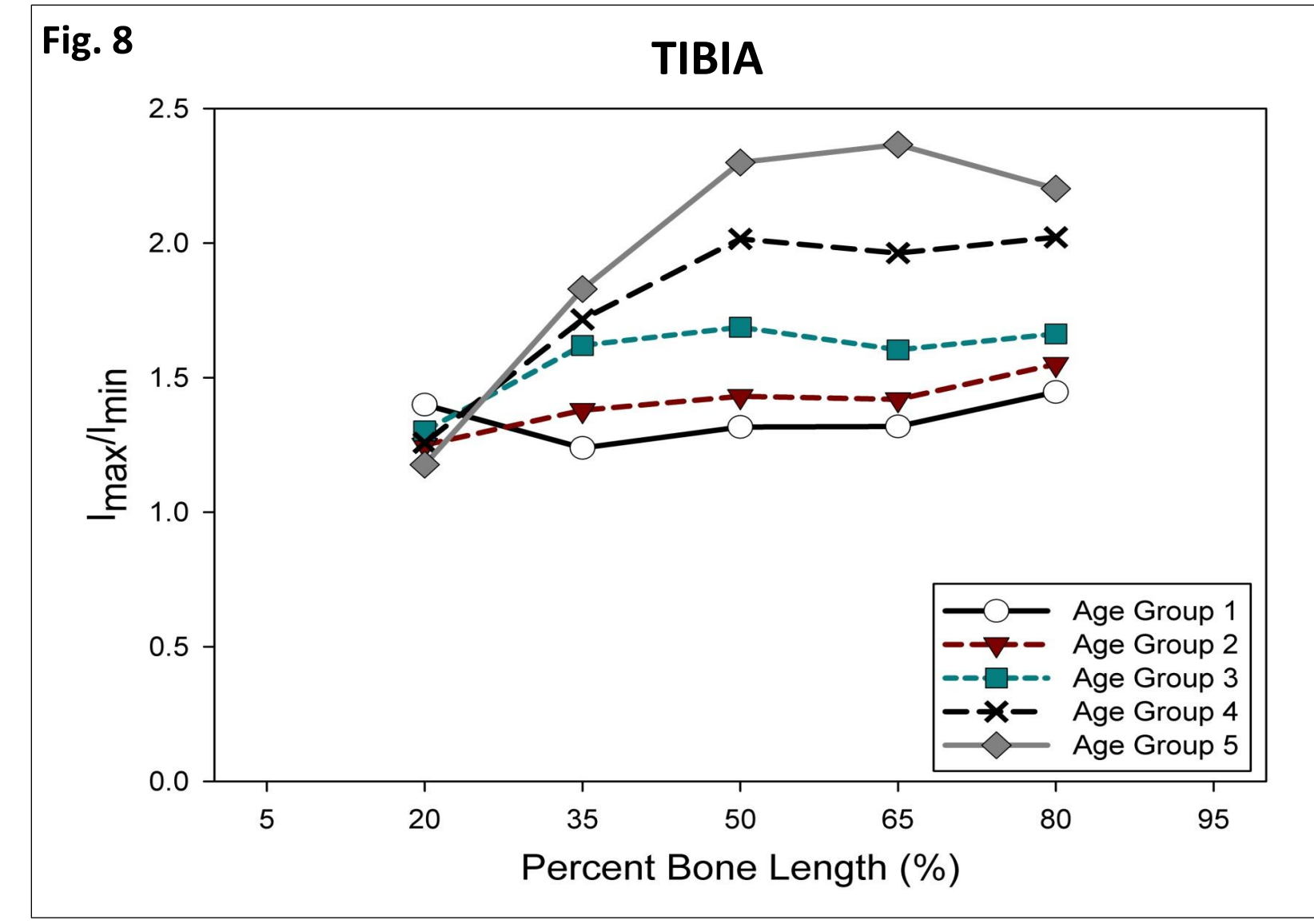


**Fig 6.** Graph of sector radius measurements (scale in mm). Example is a 16.5 year-old at the 80% tibia slice.



**Figs 7 & 8.** Mean  $I_{max}/I_{min}$  values by % total bone length at five locations in the diaphysis of the femur (left) and tibia (right). Lines represent each of five distinct age groups (in years: Group 1 = 0 - 1.9; Group 2 = 2 - 4.9; Group 3 = 5 - 8.9; Group 4 = 9 - 13.9; Group 5 = 14 - 18).



## DISCUSSION

- Sensitivity of morphological adaptation to locomotor forces is heterogeneous throughout the diaphysis of the tibia and femur.
- Significant age-related differences in cortical morphology indicate a major limitation of current geometric scaling techniques.<sup>2, 3, 4</sup>
- According to previous studies, diaphyseal fractures in the subadult *tibia* occur most frequently in the distal third of the shaft, followed by the middle third, with the fewest occurring proximally<sup>5</sup>; diaphyseal fractures of the subadult *femur* occur most frequently in the midshaft, followed by the distal region.<sup>6</sup>
- Most common fracture sites correspond to smallest  $I_{max}$  values found in this study, indicating that the femur and tibia tend to fracture at sites of least bending rigidity.

## CONCLUSIONS

- Structural response to mechanical use is age- and site-specific in the femur & tibia.
- Nuances of developmental timing and spatial variability of long bone morphology can contribute to refinement of geometric scaling techniques for child injury biomechanics research.
- Future research should combine age- and site-specific morphometrics with experimentally-derived subadult injury threshold data.

## REFERENCES

- J. Ash, Y. Abdellilah, J. Crandall, D. Parent, C. Sherwood, D. Kallieris. 2005. Comparison of Anthropomorphic Test Dummies with a Pediatric Cadaver Restrained by a Three-point Belt in Frontal Sled Tests. Proceedings of the 21st International Technical Conference on the Enhanced Safety of Vehicles.
- R.H. Eppinger, J.H. Marcus, R.M. Morgan. 1984. Development of Dummy and Injury Index for NHTSA's Thoracic Side-Impact Protection Research Program. Society for Automotive Engineers, Technical Paper.
- H.J. Mertz. 1984. A Procedure for Normalizing Impact Response Data. Society for Automotive Engineers, Technical Paper.
- H.J. Mertz, P. Prasad, A.L. Irwin. 1997. Injury Risk Curves for Children and Adults in Frontal and Rear Collisions. Society for Automotive Engineers, Technical Paper.
- E.S. Hart, B. Luther, B.E. Grottkau. 2006. Broken Bones: Common Pediatric Lower Extremity Fractures – Part III. Orthopaedic Nursing 25(6):390-407.
- R. Schwend, C. Werth, A. Johnston. 2000. Femur Shaft Fractures in Toddlers and Young Children: Rarely from Child Abuse. J Ped Ortho 20(4):475-481.

## ACKNOWLEDGMENTS

This research was supported by NSF grant BCS-1028904 (JHG, TMR)

The authors thank Amanda Agnew and Laura Boucher for their helpful comments and suggestions.